Mm-Wave MIMO Channel Modeling and User Localization Using Sparse Beamspace Signatures

A Project Report

submitted by

PATRUNI HARISH

in partial fulfilment of the requirements
for the award of the degree of

MASTER OF TECHNOLOGY

DEPARTMENT OF ELECTRICAL ENGINEERING
INDIAN INSTITUTE OF TECHNOLOGY MADRAS.

JUNE 2016

THESIS CERTIFICATE

This is to certify that the thesis titled **Mm-Wave MIMO Channel Modeling and User Localization Using Sparse Beamspace Signatures**, submitted by **P HARISH**, to the Indian Institute of Technology, Madras, for the award of the degree of **Master of Technology**, is a bonafide record of the research work done by him under our supervision. The contents of this thesis, in full or in parts, have not been submitted to any other Institute or University for the award of any degree or diploma.

Dr. Srikrishna Bhashyam
(Project Guide)
Professor
Dept. of Electrical Engineering
IIT-Madras, 600 036

Place: Chennai

Date: 11^{th} June 2016

ACKNOWLEDGEMENTS

I would like to express my greatest gratitude for the people who have helped and supported me throughout my project. I am grateful to my guide, Dr.Srikrishna Bhashyam, for his continuous support. This project would not have been a success without his valuable suggestions and insights.

I would like to thank all the faculties in the Department of Electrical Engineering for teaching me with such patience which has helped me during my project work and in my studies.

I would like to thank my family, I am indebted to them forever for their never ending support and for giving me the freedom to make the decisions in my life.

Finally I would like to thank all my friends without whom my life would not have been memorable.

ABSTRACT

KEYWORDS: Mm-Wave, MIMO, MS, LoS, ML .

Millimeter-wave (mm-wave) communication systems operating between 30GHz and 300GHz are emerging as a promising technology for meeting the large available bandwidth.The large amounts of bandwidth available in the millimeter (mm) wave band which enables the multiGigabit wireless networks with indoor and outdoor applications.The carrier wavelengths in this band are an order of magnitude smaller than the existing cellular and WiFi systems and that is resulting in a different propagation geometry.Omnidirectional transmission is infeasable because the propagation loss at smaller wavelengths is more.So the highly directive transmission and reception with electronically steerable beams can be achieved using compact antenna arrays.

In contrast to the rich scattering environment at lower frequencies, a smaller number of paths are dominant for directional mm-wave communication links. In this project work we study, the developed model (8) for sparse mm-wave MIMO channels and proposed approach to exploit the second order channel characteristics as a function of the mobile station (MS) position. Unlike the most existing methods, line-of-sight (LoS) propagation is not mandatory and the proposed approach takes care of the information provided by non-line-of sight (NLoS) paths. Beamspace channel sparsity is exploited for developing a low-dimensional maximum likelihood (ML) classifier that delivers near optimal performance with reduced complexity compared to other conventional designs.Simulation results illustrate the impact of physical environment,grid resolution, and MIMO dimensions on localization performance.

TABLE OF CONTENTS

LIST OF TABLES

LIST OF FIGURES

ABBREVIATIONS

BS	Base Station
MS	Mobile Station
AoA/AoD	Angle Of Arrival/Angle Of Departure
DFT	Discrete fourier transform
ULA	Uniform Linear Array
MIMO	Multiple Input Multiple Output
TX/RX	Transmitter/Receiver
LOS	Line Of Sight
NLOS	Non Line Of Sight
SNR	Signal to Noise Ratio
ML	Maximum Likelihood classifier

NOTATION

$\mathbf{N}_r$	Number of antennas at base station
$\mathbf{N}_t$	Number of antennas at mobile station
α_t/α_r	Angle of departure/Angle of arrival
$\mathbf{a}_{MS}$, $\mathbf{a}_{BS}$	array response vectors at MS and BS
M_k	channel sprsity mask for the k^{thcell}
H	Channel matrix
ρ	Average path loss
β_l	Path loss for the l^{th} path
ϕ_l	Path phase for the l^{th} path
Gt	Transmitter Antennas gain
Gr	Receiver Antennas gain
Pe	Probability of Error

CHAPTER 1

INTRODUCTION

1.1 Introduction

The rapid increase in the demand of consumer wireless devices is leading to exponential increase in data rates and so creating a problem of spectrum crisis at the current operating wireless frequecies.At the existing frequencies small cell technology is being explored for meeting the challenges by increasing the spatial re-use of the limited spectrum.And MIMO techonologies are important in for interference management and increasing the spectral efficiency.To increase the current data rates to the thousand fold we employ Mm-wave phenomenon with MIMO channel communication.we predict in the next decades data rates will be on the order of GiGaBytes,due to large available bandwidths as well as the high-dimensional MIMO operation.

Mm-wave systems offers unique opportunities for enabling high data rate wireless communication.First, it opens up the large portions of unused spectrum that can support orders of magnitude large bandwidths (10s of GHz) compared to existing systems.Second, exploiting the spatial dimension is particulary promising.Due to the highly directional nature of propagation, line-of-sight (LoS) propagation plays an important role at mm-wave communication.Basically mm-wave communication is dominated by the LoS paths and a very few dominant single-bounce NLoS paths.So it results in sparse channel characteristics.

1.2 Objective of The Project Work

In mm-wave communication exploiting the spatial dimension is particularly promising. For a given antenna size **A** the small wavelength, λ,

leads to a dramatic increase in the dimension of the spatial signal space, $\mathbf{n} = \frac{4\mathbf{A}}{\lambda^2}$.In addition to creating narrow, high gain beams,the high dimensional spatial signal space can be exploited by multiple-input multiple-output (MIMO). Due to the directive nature of communication LoS propagation is dominated, and few single bounce NLoS propagation paths provides the channel information in mm-wave.So the channel is having a sparse beamspace masks.

We study the developed model (8) for sparse MIMO channels, appropriate for mm-wave frequencies, and the proposed approach for mobile station (MS) localization based on the changes in the secon-order statistics and sparsity patterns of the beamspace MIMO channel matrix as a function of MS position. Most existing techniques focus on the information provided by the LoS path, including angle of arrival (AoA), time difference of arrival (TDoA) or the received signal strength (RSS).

The directional LoS path and few single bounce NLoS paths provides sparse channel MIMO matrix. So this channel sparse masks exploits the low rank MIMO channel matrix. The sparsity of the channel matrix is exploited to develop a low-complexity ML classifier that delivers near optimal performance with dramatically reduced complexity.

1.3 Organization of Thesis

Chapter 2 Presents detailed description of modeling and analysis of millimeter wave systems. This chapter also describes the MIMO architecture used in mmwave communication systems. And channel modeling of Mm-wave beamspace communication is discussed in detail.

Chapter 3 Introduces how the channel sparse information is varying among the channels. And we preented a noisy measurement channel and empirical channel statistics. Given the description about how user localization can be done by ML classifier, and low dimensional classifier exploits the channel sparse information. In the section titled' simulation and results' we discuss the results obtained via monte-carlo simulations using matlab.

Chapter 4 summarizes the project work.

CHAPTER 2

BEAMSPACE MIMO SYSTEM MODEL

2.1 Sampeld MIMO System Representation

Consider a linear antenna of length **L**. If the aperture is sampled with critical spacing, d = $\frac{\lambda}{2}$ where λ is the critical wavelength. The critical spaced sampling results in there is no loss of information. The sampled points on the aperture are equivalent to a N-dimensional Uniform linear array (**ULA**) of antennas, where N = $\frac{2\mathbf{L}}{\lambda}$ is the maximum number of spatial modes supported by the Uniform linear array **ULA**.

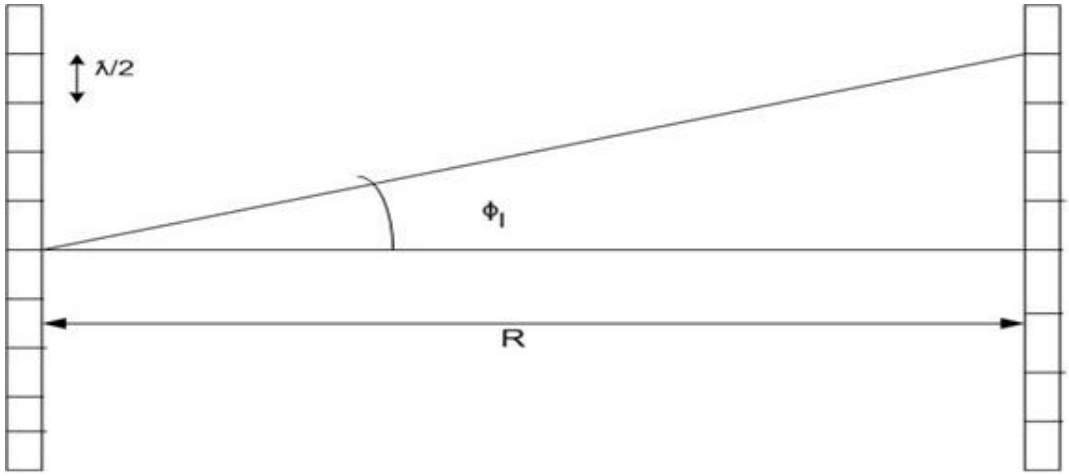

Figure 2.1: Illustration of LoS channel.

The beamforming gain or antenna gain is proportional to number of spatial modes that is, lets say **G** is the gain of the beamforming antenna then antenna gain **G** = $\frac{2\pi N}{\lambda}$. Conventional **MIMO** system with Uniform linear antennas (**ULAs**) at the transmitter and the receiver can be modeled as

$$\mathbf{r} = \mathbf{H}\mathbf{x} + \mathbf{w} \tag{2.1}$$

where **H** is the $N_R \times N_T$ aperture domain channel matrix representation coupling between the transmitter and receiver Uniform linear antenna (**ULA**) elements, **x** is the $N_T \times 1$ dimensional transmitted signal vector, **r** is the $N_R \times 1$ dimensional received signal vector, and **w** $\sim$ **CN (O,I)** is the $N_R \times 1$ dimensional vector of unit variance additive white gaussian noise.

2.2 Beamspace MIMO System Representation

The conventional Multiple input Multiple output system **(MIMO)** operates in MHz frequency range, so it can't be used to transmit the mm-wave frequencies directly. So beamforming is the new mm-wave technique which is going to be applied at the both transmitter and receiver. Modulation of data onto orthogonal basis waveforms is a fundamental concept in communication theory, and these orthogonal spatial beams form an optimal basis for the spatial dimension (1). The Beamspace **MIMO (B-MIMO)** system representation is obtained from (2.1) via fixed beamforming at the transmitter and receiver. The beamforming can be done at the transmitter and receiver by using beamspacing matrices as shown in the fig. 2.2.

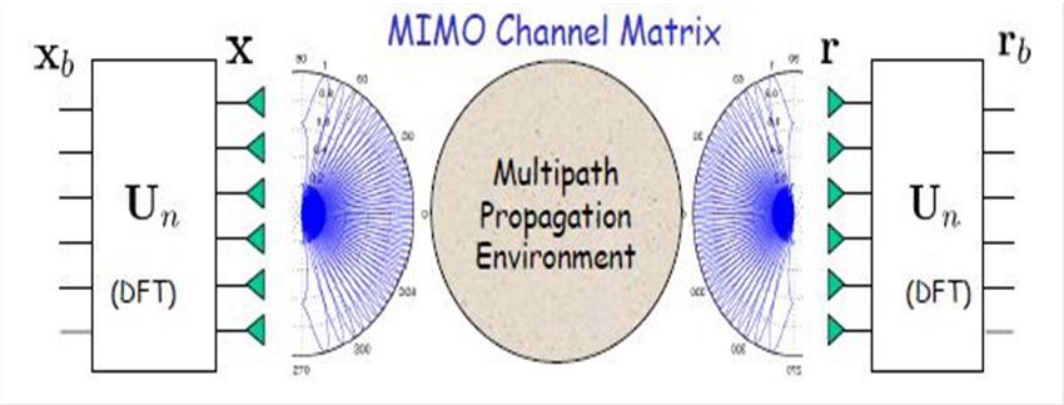

Figure 2.2: Beamspace MIMO system representation.

Each column of the beamspacing matrices, $\mathbf{U_{N_T}}$ and $\mathbf{U_{N_R}}$, is an array

steering / response vector at a specified angle (1). For a critically spaced Uniform linear array **ULA**, a plane wave is propagating in the direction of angle ϕ see fig. 2.1 corresponds to a spatial frequency, $\theta = 0.5\sin(\phi)$, and the corresponding array steering / response (column) vector is given by (2).

$$\mathbf{u_n}(\theta) = [\mathbf{e}^{-\mathbf{j2}\pi\theta\mathbf{i}}]_{\mathbf{i}\epsilon\mathbf{I(n)}} \tag{2.2}$$

where I(n) = {j : j=1,2,.....,n} is a set of indices for a given dimension n. The columns of $\mathbf{U_n}$ correspond to n fixed spatial frequencies/angles with uniform spacing $\Delta\theta_o$ = $\frac{1}{n}$.

$$\mathbf{U_n} = \frac{\mathbf{1}}{\sqrt{\mathbf{n}}}[\mathbf{u_n}(\mathbf{\Delta}\theta_\mathbf{o}\mathbf{i})]_{\mathbf{i}\epsilon\mathbf{I(n)}} \tag{2.3}$$

which represent n orthogonal beams, with beamwidth $\Delta\theta_o$, that cover the entire horizon ($\frac{-\pi}{2} \leq \phi \leq \frac{\pi}{2}$) and form a basis for the n-dimensional spatial signal (2). In fact U_n is a unitary discrete Forier transform **(DFT)** matrix. The overall beamspace representation is obtained from Eq 2.1 as

$$\mathbf{r_b} = \mathbf{H_b x_b} + \mathbf{w_b}, \mathbf{H_b} = \mathbf{U^T_{b,R} H U_{b,T}} \tag{2.4}$$

where $\mathbf{x_b}$ = $\mathbf{U_{b,T}} * \mathbf{x}$ = $[x_b(1), x_b(2), ...x_b(N_T)]^T$ is the transmitted beam space signal vector, $\mathbf{r_b}$ = $\mathbf{U^T_{b,R}} * \mathbf{r}$ = $[r_b(1), r_b(2), ...r_b(N_R)]^T$ is the received beam space signal vector, $\mathbf{H_b}$ is the $\mathbf{N_R} * \mathbf{N_T}$ beamspace channel matrix that represents the coupling between the spatial beams at the transmitter and receiver as shown fig. 2.2. $\mathbf{U_{b,T}}$ is the $\mathbf{N_T} * \mathbf{N_T}$

transmit beamforming matrix, $\mathbf{U_{b,R}}$ is the $\mathbf{N_R} * \mathbf{N_R}$ the receive beamforming matrix, and $\mathbf{w_b} = \mathbf{U_{b,R}^T w}$ is the $\mathbf{N_R} * \mathbf{1}$ beamspace noise vector. Since $\mathbf{U_{b,T}}$ and $\mathbf{U_{b,R}}$ are unitary **DFT** matrices, $\mathbf{H_b}$ is a 2D DFT of H and thus a completely eqivalent representation of H (1).

2.3 Beamspace MIMO Channel Modeling

From electromagnetic wave theory, we know that signals experience larger attenuation at higher frequencies. As millimeter wave frequencies are too high, in order of 100GHz, large number of antenna elements are deployed at Tx and Rx to ensure highly directive signal transmission and overcome the attenuation. However, due to small size and closely packed antenna elements, we observe high correlation between the responses of the antenna elements employed within the array. Consider a frequency non-selective MIMO system equipped with one-dimensional uniform uniform linear array **(ULA)** of $\mathbf{N_T}$ number of antennas and $\mathbf{N_R}$ number of antennas at the Mobile station (MS) and Base station (BS) respectively.

In general the channel is posessed with many scatters in the environment. So the coupling channel between each Mobile station (MS) and Base station (BS) is decided by scattering phenomenon like the scattering path attenuation and phase.Due to the quasi optical nature of propogation, mm-wave communication is dominated by LoS paths and few dominant single-bounce NLos paths, that results in a sparse channel characteristics (3).Since mmWave channels are expected to have limited scattering, we adopt a geometric channel model with N_p scatterers. Each scatterer

is further assumed to contribute single propagation path between the BS and MS. Under this model, the MIMO channel can be accurately modeled as

$$\mathbf{H} = \sqrt{\frac{N_T N_R}{\rho}} \sum_{l=0}^{\mathbf{N_p}} \beta_{\mathbf{l}} \mathbf{e}^{\mathbf{j}\phi_{\mathbf{l}}} \mathbf{a_r}(\theta_{\mathbf{r,l}}) \mathbf{a_t^H}(\theta_{\mathbf{t,l}}) \tag{2.5}$$

where N_p denotes the number of propogation paths, $\theta_{r,l}$ and $\theta_{t,l}$ are the angles seen by the Base Station(BS) and Mobile Station(MS), respectively, and β_l and ϕ_l represent the amplitude and phase for the l-th path. The LoS path corresponds to l=0. The response vector $a_r(\theta_{r,l})$ and steering vector $a_t(\theta_{t,l})$ are given by

$$a_r(\theta_{r,l}) = \frac{1}{\sqrt{N_R}}[a_{r,1}(\theta_{r,l})], ..., a_{r,N_R}(\theta_{r,l})] \tag{2.6}$$

$$a_t(\theta_{t,l}) = \frac{1}{\sqrt{N_T}}[a_{t,1}(\theta_{t,l})], ..., a_{t,N_T}(\theta_{t,l})] \tag{2.7}$$

The elements of response/steering vector and normalized spatial angles $\theta_{r,l}$ and $\theta_{t,l}$ are given by

$$\begin{aligned} \mathbf{a_{r,i}}(\theta_{\mathbf{r},l}) &= \mathbf{e}^{-\mathbf{j2}\pi\theta_{\mathbf{r},l}(\mathbf{i-1})} \\ \mathbf{a_{t,i}}(\theta_{\mathbf{t},l}) &= \mathbf{e}^{-\mathbf{j2}\pi\theta_{\mathbf{t},l}(\mathbf{i-1})} \end{aligned} \tag{2.8}$$

with $\theta_{r,l}$ = $\frac{d_r \sin(\alpha_{r,l})}{\lambda}$, $\theta_{t,l}$ = $\frac{d_t \sin(\alpha_{t,l})}{\lambda}$ and where λ is the wavelength, $\alpha_{r,l}$ and $\alpha_{t,l}$) are the physical angles and $d_r$and d_t the antenna spacing at the Base station (BS) and Modile station (MS), respectively. And we for the no loss of information at the Transmitter and Receiver, we assume $d_r = d_t = \frac{\lambda}{2}$.

According to the physical model (2.5), there are four parameters for

each path: $\mid \beta \mid$, ϕ_l, $\theta_{r,l}$, $\theta_{t,l}$. These parameters vary depend on the Mobile station (MS) location relative to the scatterers position. In this thesis work we consider the LoS path and single-bounce NLoS scattering paths since higher-order bounces suffer too much attenuation at mm-wave frequencies (4).

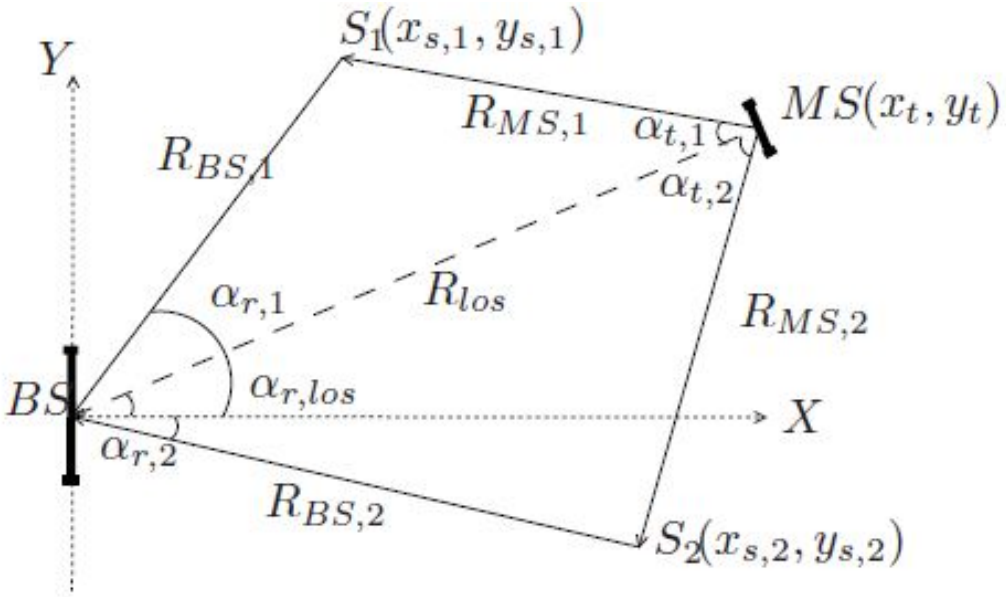

Figure 2.3: Geometric relation between BS and MS.

The geometrical relation between the BS and MS relative to the propagation paths is shown in fig. 2.3. We fix the BS position as the origin, and the broadside direction as positive x-axis. The MS is always assumed facing the BS. The Scattering objects are located between the BS and the MS in the area: $\{ (x_s, y_s) : 50m \leq x \leq 150m, -50m \leq y \leq 50m \}$.

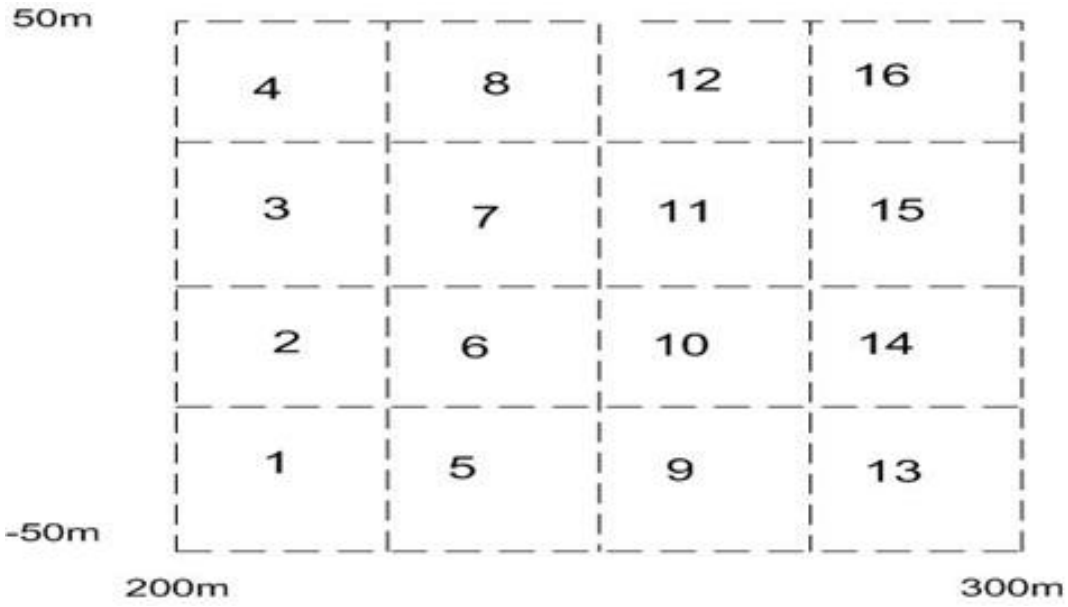

Figure 2.4: Cell numbering.

As shown in fig. 2.4 , we define the moving area for MS as { (x_t, y_t) : $200m \leq x \leq 300m, -50m \leq y \leq 50m$} and split the whole area into 16 disjoint cells $(25mX25m)$ for the default case.

2.3.1 Angle of Departure (AoD) and Angle of Arrival (AoA):

Since the MS is always facing the BS, for the LoS path $(l = 0)$, the AoD at the MS is always zero $(\alpha_{t,los} = 0)$, and the AoA at the BS $(\alpha_{t,los})$ is defined relative to the x-axis. For a particular NLoS scattering path $(l = 1, ..., N_p)$, we define the AoD $(\alpha_{t,l})$ as the angle between the outgoing wave direction (from the MS) and LoS path direction, and the AoA $(\alpha_{r,l})$ at the BS as the angle between scattered wave direction and the positive x-axis. The AoDs and AoAs, {$(\alpha_{t,l}, \alpha_{r,l})$ }, can be computing by using the geometrical by using the geometrical relationship between the MS and scatterer locations relative to the BS; fig. 2.3 The normalized AoAs and AoDs are computed via (2.8).

2.3.2 Path Amplitude and Phase:

For a given MS position, (x_t, y_t), the phase for the LoS path $(l = 0)$ is given by

$$\phi_l(x_t, y_t) = \phi_{los}(x_t, y_t) = \frac{2\pi R_{los}}{\lambda} = \frac{2\pi\sqrt{x_t^2 + y_t^2}}{\lambda} \tag{2.9}$$

Similarly, for the same MS position, and for a given scatterer position, (x_s, y_s), the phase for the corresponding NLoS path $(l = 1, 2....., N_p)$ can be computed as

$$\phi_l(x_t, y_t; x_{s,l}, y_{s,l}) = \frac{2\pi(R_{BS,l} + R_{MS,l})}{\lambda} \tag{2.10}$$

Where $R_{BS,l} = \sqrt{x_{s,l}^2 + y_{s,l}^2}$ is the distance from the BS to the scatterer and $R_{MS,l} = \sqrt{(x_t - x_{s,l})^2 + (y_t - y_{s,l})^2}$ is the distance from the BS to the scatterer to the MS; see fig. 2.3.

The path loss for the LoS path $(l = 0)$ is given by: $\mid \beta_o \mid^2 = G_t G_r (\frac{\lambda}{4\pi R_{los}})^2$, and the path for single-bounce NLoS paths $(l \geq 1)$ can be calculated as (5)

$$\mid \beta_l \mid^2 = \frac{P_{r,l}}{P_{t,l}} = \frac{G_t G_r \sigma}{(4\pi)^3} (\frac{\lambda}{4\pi R_{BS,l} R_{MS,l}})^2 \tag{2.11}$$

where $P_{r,l}$ and $P_{t,l}$ are the power of received and transmitted signals,G_r and G_t are the antenna gains of BS and MS arrays, respectively, and σ represents the radar cross section which depends on the properties of scatterer and scattering angles. In simulations, we simply set σ = 1 for NLoS paths. Furthermore, prompted by recent measurements (6), we scale the LoS vs NLoS gains so that the NLoS path gains are 5-10dB weaker than the LoS path gain.

CHAPTER 3

SPARSE BEAMSPACE CHANNEL STATISTICS AND USER LOCALIZATION

3.1 Introduction

Mm-wave beam communication is operating in the GHz frequency range to acquire the maximum data rates, so that it can meet today's Bandwidth requirement. Since the wavelength is too small path attenuation is high. So the beamspace communication is employed to transmit it to the far distance. With this beamspace modulation the directivety of spatial beam is high, so the LoS path is more dominant and few NLoS single bounce paths will present. Now The Beamspace MIMO channel is having a few channel sparsity masks. By exploiting those channel sparsity masks we can reduce the complexity of Transceiver, and the number of communication modes are now less than that of the number of propagation modes.

In this chapter we firstly present channe statistics and and channel sparsity masks for each mobile station. We assume that we measured the channel with noisy measurements. And aslo we study the empirical channel covariance statistics. Also we analyse the Maximum likelihood classifier performance with full dimension of channel matrix and we present a low-dimensional classifer by exploiting the channel sparse information.

We present the encouragive MATLAB simulation results at the end of the chapter. Since the measured channel distribute as gaussian probabilty

function using the Maximum likelihood classifier we estimate the user position. We Considering the various factors like Environment,MIMO dimensions, and cell sizes. The simulation results compare the performance of ML classifier and Low dimensional classifier with reduced dimension.

3.2 SPARSE BEAMSPACE CHANNEL STATISTICS

3.2.1 Channel Statistics and Sparsity Masks

We construct a $N_r N_t * 1$ column channel vector $h_b = vec(H_b)$. From the column channel vector we deduce the beamspace channel covariance matrix is Σ_b = $E[h_b h_b^H]$. Hb is sparse due to the mm-wave propagation characteristics and so the channel power is concentrated in a low-dimensional sub-matrix. Let $\Sigma_{b,k}$ denote the channel covariance matrix for the kth cell and the total channel power is σ_k^2 = trace($\Sigma_{b,k}$). For each cell, define the following sets of indices as the channel sparsity masks, M_k, that capture most of the channel power:

$$M_k = \{i : \Sigma_{b,k}(i,i) \geq \gamma_k \arg\max_i \Sigma_{b,k}(i,i)\}, \tag{3.1}$$

$$M = \bigcup_{k=1,.....K} M_k \tag{3.2}$$

Where threshold γ_k is chosen so that M_k captures a specified (large) fraction $\eta_k \in$ [0,1] of the channel power

$$\sum_{i \in M_k} \Sigma_{b,k}(i,i) \geq \eta_k \sigma_k^2. \tag{3.3}$$

M_k and M represent the channel sparsity masks or signatures for the k^{th} cell and entire area. For the k-th cell, the lowdimensional channel covariance matrix is defined as

$$\widetilde{\Sigma}_{b,k} = [\Sigma_{b,k}(i,j)]_{i,j \in M_k} \tag{3.4}$$

3.2.2 Measurement Model and Empirical Channel Statistics

In practice, channel statistics are estimated from noisy measurements. Generally using the received power of mobile station by assuming the log-loss path model as the channel modeling we estimate the Angles of Arrival, Angles of Departure and attenuation of scatteres by stastical estimation approach. But, In this thesis we assume that we measure the channel model with the noisy measurements. We consider the following model for the beamspace channel measurements:

$$h_{bn} = \sqrt{\epsilon} h_b + w_b \tag{3.5}$$

where $h_{bn}$is the noisy measurement vector, $w \sim CN(0, I)$ denotes the noise vector, and ϵ represents the signal-to-noise ratio (SNR). In (3.5), h_b hb represents a normalized channel vector so that $\sigma^2 = E[\|h_b\|^2] = 1$. We are doing this because we want to eliminate the influence of channel power on classification performance. Our focus is mainly on the influence of channel power over the sparsity masks. Thus, for the k-th cell we have:

$$\Sigma_{bn,k} = E[h_{bn} h_{bn}^H] = \frac{\epsilon}{\sigma^2} \Sigma_{b,k} + I \tag{3.6}$$

To estimate the user location we use the empirical channel stastics of that particular k-th cell by taking N_{sp} sample postions,$\{(x_{r,i}, y_{r,i}) : i = 1, ...N_{sp}\}$, uniformly placed in the k-th cell and use the empirical covariance matrix:

$$\widehat{\Sigma_{b,k}} = \frac{1}{N_{sp}} \sum_{i=1}^{N_{sp}} h_b(x_{r,i}, y_{r,i}) h_b^H(x_{r,i}, y_{r,i}) \tag{3.7}$$

Where the channel vectors for different positions are generated using the physical model (2.5). Note that $E[\widehat{\Sigma_{b,k}}] = \Sigma_{b,k}$.

3.3 USER LOCALIZATION ALGORITHM

We now formulate the user localization problem, characterize the ML classifier, and low-dimensional classifier based on channel sparsity masks.

3.3.1 Maximum Likelihood Classifier

Suppose that the Mobile Station is located in one of the K disjoint cells with equal probability The localization problem can be seen as a K-ary hypothesis testing problem

$$H_k : h_{bn} \sim CN(0, \Sigma_{bn,k}) \tag{3.8}$$

where h_{bn} is a noisy channel measurement (3.5) and $\Sigma_{bn,k}$ is the covariance matrix for the k^{th} cell as in (3.6). The optimal ML classifier chooses the cell as (7):

$$C(h_{bn}) = \arg \max_{k=1,.....,K} p_k(h_{bn}) \tag{3.9}$$

where $p_k(h_{bn})$ is the probability density function under H_k:

$$p_k(h_{bn}) = \frac{1}{\pi^{NrNt}\det(\Sigma_{bn,k})} e^{-h_{bn}^H \Sigma_{bn,k}^{-1} h_{bn}} \tag{3.10}$$

Using log-likelihood, the classifier can be simplified as

$$C(h_{bn}) = \arg\min_k [\log(\det(\Sigma_{bn,k})) + h_{bn}^H (\Sigma_{bn,k})^{-1} h_{bn}] \tag{3.11}$$

3.3.2 Low-dimensional Classifier

As the channel is having few sparsity masks, it can be exploited to analyse the low-dimensional classifier performance. The low-dimensional classifier exploits the sparsity patterns and operates on the low-dimensional channel vector defined by $M : \widetilde{h_{bn}} = [h_{bn}(i)]_{i \in M}$. For the k th cell the empirical channel covariance matrix with respect to the Signal to noise ratio is,

$$\widetilde{\Sigma_{bn,k}} = [\Sigma_{bn,k}(i,j)]_{i,j \in M_k} \tag{3.12}$$

Using the log-likelihood the low dimensional classifier performance can be analysed as

$$C(h_{bn}) = \arg\min_k [\log(\det(\widetilde{\Sigma}_{bn,k})) + \widetilde{h}_{bn}^H (\widetilde{\Sigma}_{bn,k})^{-1} \widetilde{h}_{bn}] \tag{3.13}$$

3.3.3 Classifier Performance Evaluation

We evaluate the classifier performance in terms of the average error probability:

$$P_e = \frac{1}{k}\sum_{k=1}^{K} P_{e,k}, P_{e,k} = P(C(h_{bn} \neq k|H_k)) \tag{3.14}$$

where $P_{e,k}$ is the conditional error probability under H_k. We are using the Monte Carlo MATLAB simulations to estimate P_e.

3.4 Simulation and Results

We present three sets of numerical results. The first set shows the beamspace channel masks for different cells. The second shows impact of physical environment and system parameters on the localization performance. Finally, the performance of low-dimensional classifiers is discussed. We have used matlab for the purpose of monte carlo simulations. The parameters used for the modeling and simulation are as mentioned in the table.

Table 3.1: Parameter specifications for simulation

Parameters	Values	Remarks
N_r	25	Number of antennas at BS
N_t	5	Number of antennas at MS
f	38GHz	Frequency of operation
N_{sp}	10000	Number of Sample positions in each cell
f	38GHz	Frequency of operation
γ_k	0.2,0.3,0.4	Threshould values for M_k

3.4.1 Beamspace Channel Statistics and Masks

Consider a MIMO system with N_r = 25 (BS) and N_t = 5 (MS), and antenna gains G_r and G_t that are proportional to N_r and N_t. The propagation frequency f_c is 38GHz. We partition the MS movement region R into 16 disjoint cells of size 25m x 25m, and number them as in fig. 2.4. For each cell, we calculate the path loss of NLoS paths via (2.11), and set the power of LoS path, $\mid \beta_{los} \mid^2$, 10dB larger than the average power of all NLoS paths within the cell. In each cell, we uniformly pick Nsp = 10000 sample MS positions and compute the average channel power, and covariance matrix for this cell by (3.7). This is used for generating normalized channel measurements as in (3.5). The channel sparsity masks with different threshold values are generated using (3.1).

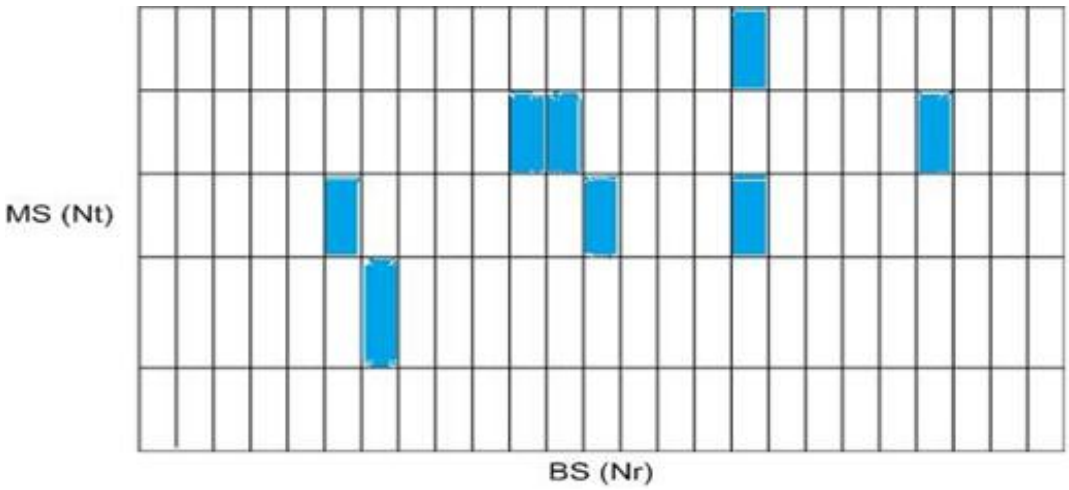

Figure 3.1: Channel sparsity mask for cell M_1.

The above fig. 3.1 shows M_k for cells 1,16 which are at corners of the MS movement area, corresponding to $\gamma_k = \gamma$ =0.1. The shaded bins represent the dominant beamspace channel entries corresponding to pairs of BS/MS beams that are strongly coupled. The mask dimensions and patterns depend on the choice of γ and the physical environment.

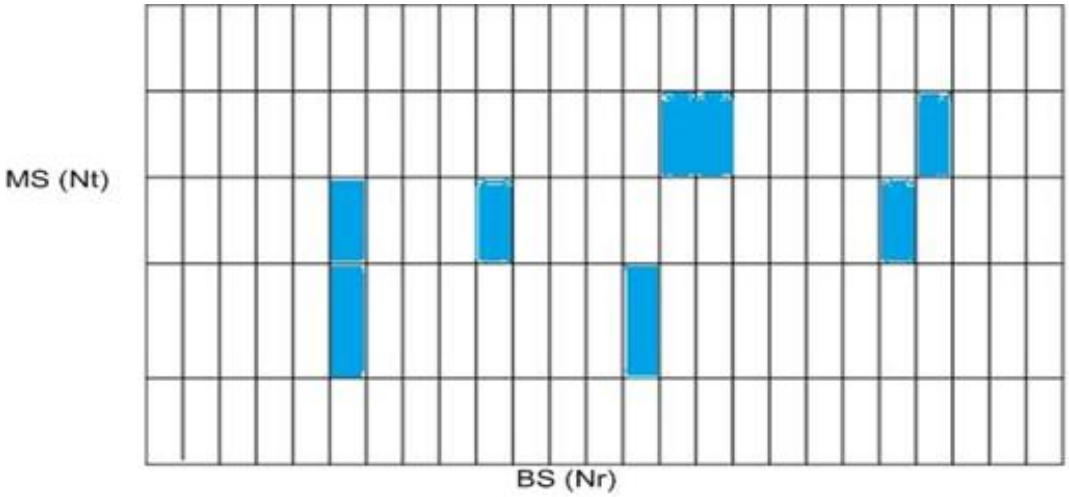

Figure 3.2: Channel sparsity mask for cell M_{16}.

3.4.2 Performance of MS localization

We have used Probability of error vs SNR to compare the performance of MS localization by varying different parameters.

In each simulation we have carried out the following steps:

1. we assume in each cell MS is moving into different locations and BS positon is fixed at origin.
2. We randomly select the scatters location for each MS position.
3. For each position in each cell we caliculate the channel matrix by using Beamspace MIMO channel modeling.
4. We unformly choose N_{sp} sample positons in each cell and estimate the empirical covariance matrix.
5. Next we determine the noisy channel measurement from the model we defined.
6. Using the log-likelihood function we maximize the channel covariance matrix for each k^{th} cell with respect to the channel measurement of the each MS postion.
7. Plotting of the probability of error vs SNR for each parameter. .

We next evaluate impact on the performance of MS localization by the physical propagation environment, cell size, and MIMO dimensions.

(A) Physical Propagation Environment:

We first discuss the impact of number of scatter paths N_p. We set the each cell size to 25m x 25m (totally 16 cells) and consider a system with $N_r = 25$ antennas at BS and $N_t = 5$ antennas at MS. We evaluate the probability of error (P_e) as a function of SNR for different values of N_p by progressively adding the scatters locations to previously locations.

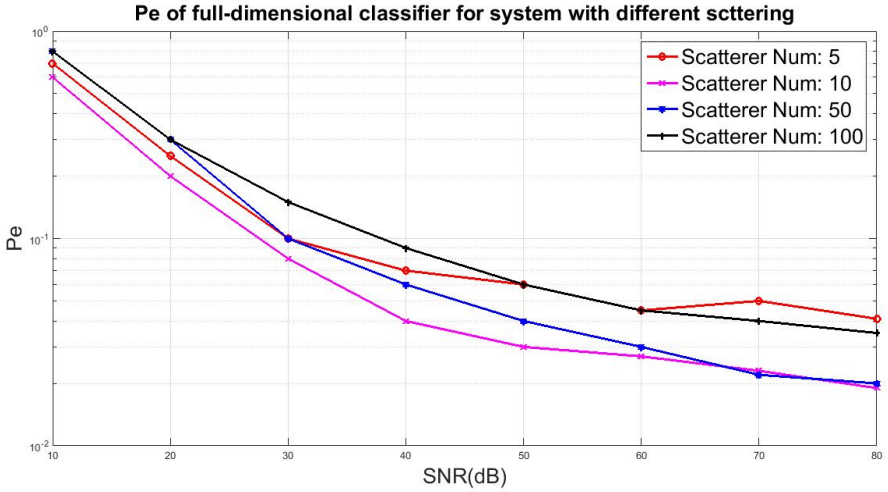

Figure 3.3: P_e for different N_p with N_r=25,$N_t = 5$

The above fig. 3.3 tells us the fact that Probability of error first decreases as N_p increases from N_p = 5 to 10, but it also gives a fact when N_p increases to 50 and 100 the Probability of error is increases. This illustrates that for a given cell dimension too many paths can degrade the performance and also as the number of scttering paths are increases the channel sparse signatures for different cells are looking similar together.

(B) MIMO Dimensions:

Now we see how the MIMO dimensions impact on the MS localization performance. In practice, increasing the number of antennas at the Mobile station is costly. So we only can increase the antennas at the base station. WE fix the MS with N_t=5 and vary N_r= 10,25,60. The below fig. 3.4 shows that systems with larger number of antennas can exploit an environment with larger number of paths for improved performance.

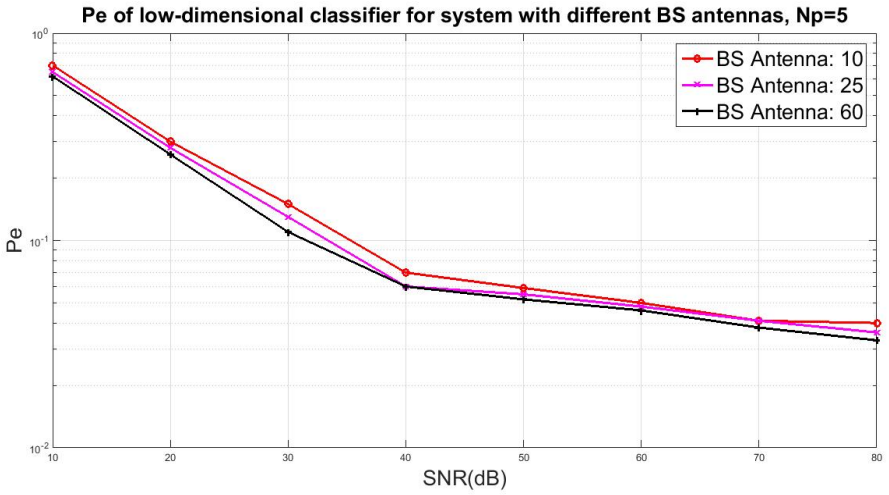

Figure 3.4: P_e for $N_t = 5$ and different N_r in an environment with N_p=5.

In fig. environment with few scatters $N_p = 5$ (very sparse environment), and increasing N_r does not change performance. However in below fig. 3.5, a much richer scatter environment N_p=100 with increasing N_r results in significantly improved performance.

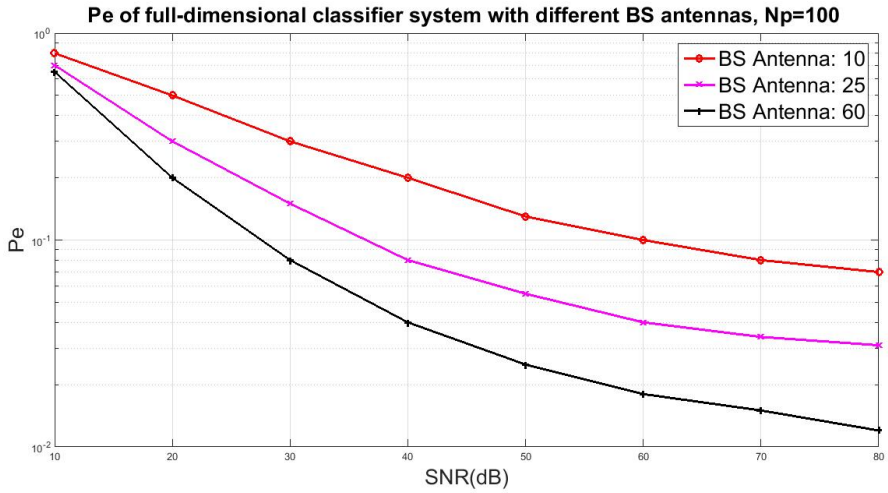

Figure 3.5: P_e for $N_t = 5$ and different N_r in an environment with N_p=100.

From both figures we can observe that the channel dimension $N_t N_r$ increases as 50,125,300 and the dimension is comparable to N_p=100. On the other hand, N_p=5 is much smaller than the channel dimension.

3.4.3 Low-Dimensional Classifier Performance

We will now see the performance of the low-dimensional classifier relative to the fulldimensional classifier in the below figures. The system dimensionality is controled by factor γ_k in (3.1).We will now examine how the low-dimensional classifier performance is changing with respect γ_k= 0.2,0.3,0.4 for two different values of N_p.

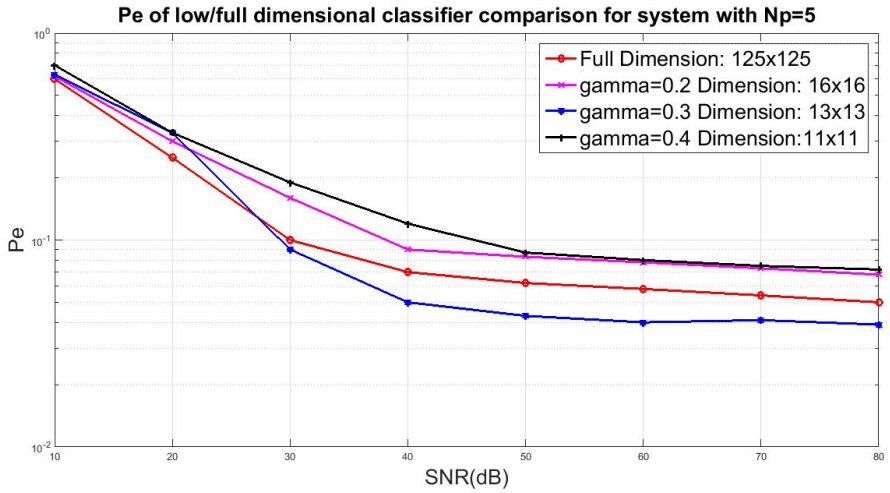

Figure 3.6: P_e of low-dimensional classifier for system with $N_r = 25$,$N_t = 5$ and $N_p = 5$.

The above fig. 3.6. is corresponds to sparse environment N_p=5 and the results shows that even the dimensionality is changed drastically from 125 to 11, there is only a litte loss of performance. And the below fig. 3.7. observes the rich scattering phenomenon with $N_p = 10$ and in this case, there is a more significant loss in performance with dimension reduction due to larger number of paths.

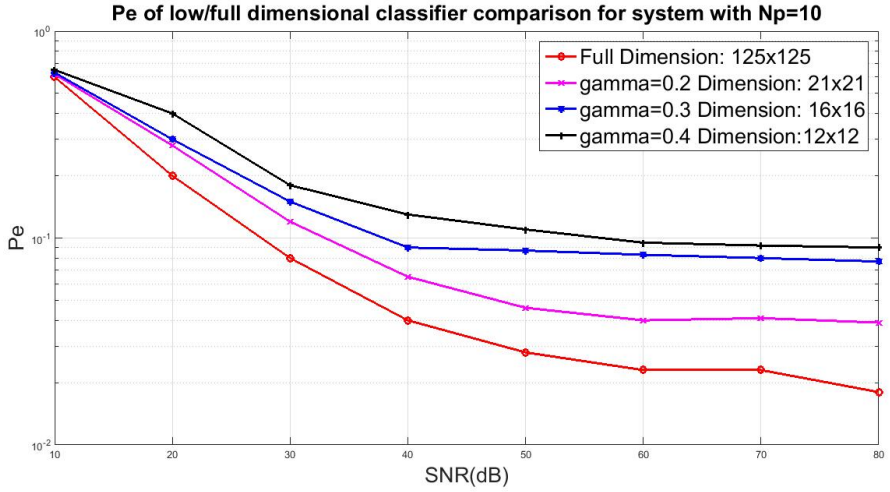

Figure 3.7: P_e of low-dimensional classifier for system with $N_r = 25$,$N_t = 5$ and $N_p = 10$.

However, still the classifier corresponds to $\gamma = 0.2$ is giving a quite

impressive performance compared with the full-dimensional. We can see that the P_e is increases by a factor of 2 when the dimension is reduced by a factor of 60, resulting in a very significant reduction in complexity.

3.5 Conclusion

The results from monte-carlo simulations of the MS localization performance and Low-Dimensional Classifier was presented in this chapter.The P_e in MS localization is observed by changing various parameters. And, we observed the comparison between Full-dimensional and Low-dimensional classifier performance. As expected low-dimensional classifier is giving a fair results with drastic change in the dimension of the system.

CHAPTER 4

CONCLUSION

4.1 Summary of The Present Work

The User localization has been done by exploiting the channel sparse characteristics. The problem of user positioning characterize ML classifier and, low-dimensional classifier by exploiting the channel sparsity masks. The two classifiers performance has compared and the simulation results obtianed via matlab monte carlo simulations. The impact of physical environment and system parameters are analyised for a full dimensional classifiers.

We have observed how the classifier performance is changing when the scattering positions are added to the previous one. As the scatters are added the all cell channel environment starts looking similar. So the P_e is increases while the number of scatters are added. And when the number of antennas are deployed more at the BS in a less sparse environment there is nothing significant achievement in the classifier performance beacuse the dimension is not comparable to the number of scatters. But, in a similar system if the Channel sparse environment N_p is comparable to the dimension, classifier achieves good performance.

We discussed the channel sparse signatures are exploited by low-dimensional classifier in a low and rich scttering environment. In a low scttering environment low-dimensional classifier achieves almost a similar performance to the full dimensional classifier with a drastic reduction in the

complexity observed by the simulation results. But in a rich scattering environment there is a significant loss in performance. However at $\gamma_k = 0.2$ the P_e increases by a factor of only 2 but the dimension reduction is by a factor of 60.

4.2 Future Scope of Work

The work presented in this thesis can be further extended in many other ways. We have considered, Uniform Linear Array of antennas in our system modeling. In future works,effect of replacing ULA with two-dimensional arrays structures can be studied. We can extend this framework to include the path delay information, and In this model we have assumed the MS is always facing BS, there may be a case when MS is intentionally points the MS towards a BS. However our future goal is to develop methods that do not require such user co-operation.

REFERENCES

[1] A. Sayeed and N. Behdad, "Continuous Aperture Phased MIMO: Basic Theory and Applications," in Proc. 48th Annu. Allerton Conf. on Communication, Control, and Computing, Sep. 29-Oct. 1 2010, pp. 1196-1203.

[2] A. M. Sayeed, "Deconstructing Multiantenna Fading Channels," IEEE Trans. Signal Processsing, vol. 50, no. 10, pp. 2563-2579, Oct. 2002.

[3] G.-H. Song, J. Brady, and A. Sayeed, "Beamspace mimo transceivers for low-complexity and near-optimal communication at mm-wave frequencies," in 2013 IEEE International Conf. on Acoustics, Speech and Signal Processing. IEEE, 2013, pp. 4394-4398.

[4] T. S. Rappaport, E. Ben-Dor, J. N. Murdock, and Y. Qiao, "38GHz and 60GHz angle-dependent propagation for cellular and peer-to-peer wireless communications," in 2012 IEEE International Conf. on Comm., 2012, pp. 4568-4573.

[5] A.Goldsmith, Wireless Communications. CambridgeUniv. Press,2006.

[6] T. S. Rappaport, E. Ben-Dor, J. N. Murdock, and Y. Qiao, "38GHz and 60GHz angle-dependent propagation for cellular and peer-to-peer wireless communications," in 2012 IEEE International Conf. on Comm., 2012, pp. 4568-4573.

[7] S. M. Kay, Fundamentals of Statistical Signal Processing: Estimation Theory, 1993, vol. 1.

[8] Hua Deng ,Akbar Sayeed "Mm-wave MIMO channel modeling and user localization using sparse beamspace signatures", Conference Paper.June 2014,DOI: 10.1109/SPAWC.2014.6941331 Conference: 2014 IEEE 15th International Workshop on Signal Processing Advances in Wireless Communications (SPAWC).